Influence of the spontaneous optical emission factor β on the first-order coherence of a semiconductor microcavity laser

S. Ates,[1,*] C. Gies,[2] S. M. Ulrich,[1] J. Wiersig,[2] S. Reitzenstein,[3] A. Löffler,[3] A. Forchel,[3] F. Jahnke,[2] and P. Michler[1]
[1]*Institut für Halbleiteroptik und Funktionelle Grenzflächen, Universität Stuttgart, D-70569 Stuttgart, Germany*
[2]*Institut für Theoretische Physik, Universität Bremen, D-28334 Bremen, Germany*
[3]*Lehrstuhl für Technische Physik, Universität Würzburg, D-97074 Würzburg, Germany*
(Received 16 September 2008; published 22 October 2008)

A systematic experimental and theoretical study of first-order coherence properties of high-β quantum-dot micropillar lasers is presented. A nonlinear increase in the coherence length is found in the transition regime from spontaneous to dominantly stimulated emission. This increase is accompanied by a qualitative change in the first-order field-correlation function $g^{(1)}(\tau)$ from a Gaussian-type profile to an exponential behavior, which is in excellent agreement with a microscopic semiconductor laser theory. Our results also demonstrate a decreasing coherence length with increasing spontaneous emission coupling β, thus raising questions about the practicability of high-β lasers for device applications.

DOI: 10.1103/PhysRevB.78.155319 PACS number(s): 78.67.Hc, 42.50.Ar, 42.55.Sa, 78.55.Cr

The coherence length of radiation is one of the most fundamental properties of a laser. Its knowledge is a crucial precondition for applications in interferometry and related areas. In recent years, intense research on the fabrication and physics of micro-and nanocavity lasers has been performed due to their high potential for ultralow threshold or even thresholdless lasers.[1] These kinds of lasers, e.g., micropillar,[2–4] microdisk,[5–7] and photonic crystal[8–10] lasers, possess both small mode volumes and high-quality factors Q. Therefore, the spontaneous emission (SE) coupling factor β of a mode, defined as the ratio of SE into that mode to the total SE into all modes, can approach values close to 1. As a consequence, a high fraction of spontaneous emission (thermal light) is coupled into the lasing mode. This leads to a reduction in the laser threshold, but at the same time the light state is composed of both thermal and coherent light states. Recent photon statistics measurements demonstrated[3,10] that the regime of fully coherent light emission in microcavities is only gradually approached at pump powers well above the smooth kink in the input-output (i/o) curve, which is commonly defined as the laser threshold. First-order field-correlation measurements $g^{(1)}(\tau)$ showed a nonlinear increase in the coherence length from subthreshold to the above-threshold regime.[3,4] Furthermore, a linear increase in the coherence length above threshold was demonstrated for a photonic crystal nanocavity laser.[11]

Up to now, systematic studies of the influence of the β factor on the coherence properties of microcavity lasers are missing. In this paper, we present comprehensive experimental and theoretical investigations of the coherence properties of different high-β micropillar lasers as a function of pump power from values below to well above threshold. A rapid nonlinear increase in the coherence length is found around the laser threshold and a strong influence of the β factor on the coherence properties of the emitted light is demonstrated. We find that the maximum achievable coherence length is limited by thermal heating effects in the corresponding cavities. The measurements are compared to results of a microscopic theory for the coupled light-matter dynamics that describes the lasing properties of quantum-dot (QD) micropillars.

The micropillar structures under study have been grown by molecular-beam epitaxy on a (001)-oriented undoped GaAs substrate. A single layer of self-assembled $In_{0.30}Ga_{0.70}As$ QDs (lateral density ca. 6×10^9 cm^{-2}) serves as the active medium that is surrounded by two 130 nm GaAs barriers to form a λ cavity. Using 27 and 23 pairs of alternating AlAs/GaAs quarter-wavelength layers as the bottom and top distributed Bragg reflectors around the GaAs layers, a planar cavity structure is realized. High-quality micropillar structures with both circular and elliptical cross sections have been processed by electron-beam lithography and Ar/Cl_2 plasma-induced reactive ion etching. Detailed information about the sample and the growth processes are reported elsewhere.[3,12] In this paper, we present measurements performed on three elliptical ($\varepsilon=20\%$) micropillars with 1.8, 2.6, and 6 μm diameters.

All optical measurements on the micropillar emission characteristics have been performed on a low-temperature ($T=4$ K) confocal microphotoluminescence (μ-PL) setup. The sample was nonresonantly excited by a continuous-wave (cw) Ti:sapphire ring laser operated at 800 nm. Emission spectra were dispersed and recorded by a 0.75 m monochromator equipped with a liquid-N-cooled charge coupled device camera providing $\Delta E\approx35$ μeV spectral resolution, which is sufficient in our case, although homogeneous linewidths for single dots of only a few μeV have been reported in the literature.[13,14] Spectrally selected emission was then sent to a computer-controlled Michelson interferometer in order to perform first-order field-correlation measurements. The Michelson interferometer consists of a 50/50 nonpolarizing beam splitter and two retroreflectors orthogonal to each other. One of the retroreflectors is mounted on a feedback-controlled linear translation stage to introduce distinct differences between the arms of the interferometer. In order to record subsequent interference fringes, a single avalanche photodiode is attached to the interferometer.

It is known that the degeneracy of the fundamental mode is lifted in elliptical pillars, resulting in a pair of orthogonally polarized modes.[4,15,16] A typical linearly polarized μ-PL spectrum taken at low excitation power from a 6 μm micro-

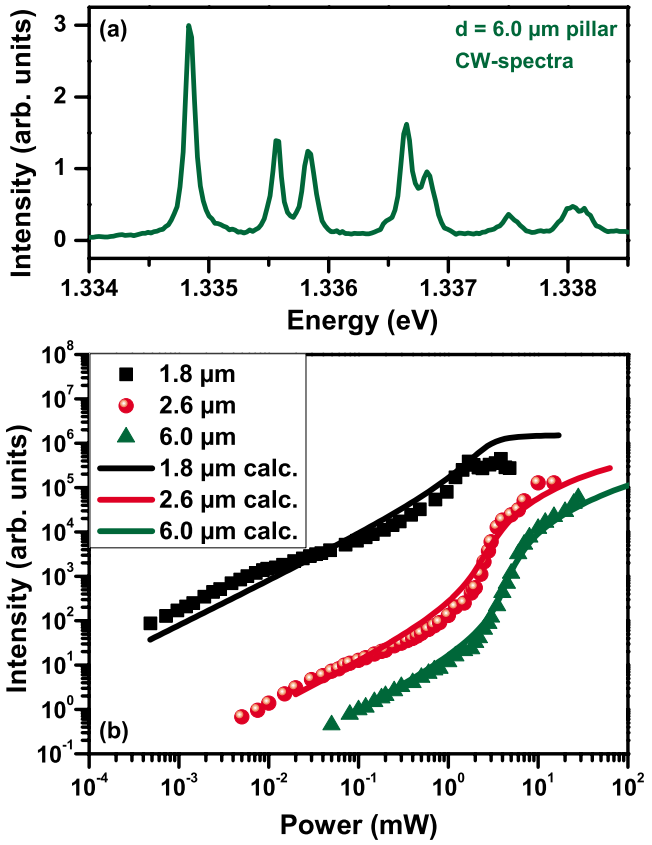

FIG. 1. (Color online) (a) A typical high-resolution linearly polarized μ-PL spectrum taken at $P=0.5$ mW from a 6 μm elliptical micropillar showing the fundamental and higher excited modes. (b) Excitation power–dependent output intensity of the fundamental-mode emission from 1.8, 2.6, and 6 μm pillars in a log-log plot under nonresonant cw-excitation conditions. The curves are shifted for clarity. Due to heating effects at high excitation conditions, the upper branch of the 1.8 μm pillar is not fully covered. Solid lines represent the calculated curves from which β is determined. Theoretical results are shifted to match the milliwatt scale of the experiment.

pillar is shown in Fig. 1(a). The fundamental mode (left peak) and higher excited modes of the micropillar can clearly be observed in the emission. All further measurements have been performed on the high-energy polarization component of the fundamental mode that dominates the emission spectra with increasing excitation power.

Figure 1(b) displays the excitation power–dependent output intensities of the fundamental mode emitted from all three micropillars on a double-logarithmic scale. An s-shaped smooth transition from spontaneous to dominating stimulated emission is observed for all pillars as expected for high-β lasers.[2,3,10] To complement our studies of microcavity lasing, we employ a semiconductor theory that has been developed to describe the emission from QDs under consideration of their semiconductor nature.[17] Despite the fact that the discrete level spectrum of QDs invites for a description via atomic models, many-body effects and Coulomb interaction cause QDs to differ from atoms in many aspects, the nonlinear source term of spontaneous emission being just one example.[18,19] With the following parameters we find a consistent overall description and an estimate of the structural parameters of the experiment. For the 6 μm pillar a number of 500 QDs (2.6 μm: 170; 1.8 μm: 80) is used, along with a total spontaneous emission time of 80 ps (2.6 μm: 55 ps; 1.8 μm: 45 ps) and a homogeneous QD broadening of $\Gamma \approx 200$ μeV. Furthermore, we consider the measured Q factors of 44 500 (6 μm), 38 000 (2.6 μm), and 20 000 (1.8 μm) which have been derived from coherence time measurements via Fourier transformation around the transparency point.[20] The β factor is used to fit the height of the jump in the i/o curves to the experiment. The results are shown as solid lines in Fig. 1(b). For the 6 and 2.6 μm pillars, we obtain β values of 0.01 and 0.03, respectively. For the smallest pillar, heating effects cause instabilities that limit the maximum excitation power. This becomes clearly visible above an excitation power of 3 mW. A β value of 0.05 has been estimated in this case by extrapolation. The observed threshold reduction with decreasing pillar diameter is due to the larger Purcell effect which enhances the SE into the laser mode by a factor of $\sim Q/V$, V being the mode volume.

The coherence properties of the fundamental-mode emission have been investigated by direct measurements of the first-order correlation function

$$g^{(1)}(\tau) = \frac{\langle b^{\dagger}(t) b(t+\tau) \rangle}{\langle b^{\dagger}(t) b(t) \rangle}, \tag{1}$$

which is here expressed in terms of quantum-mechanical averages of annihilation and creation operators b and $b^{\dagger}$ for photons in the fundamental mode. The first-order coherence describes field correlations and is, therefore, directly linked to the appearance of interference fringes in superimposed coherent light beams. A measurement of $|g^{(1)}(\tau)|$ is possible by analysis of the visibility of interference fringes observed at the output port of the Michelson interferometer according to $V(\tau) = (I_{\max} - I_{\min})/(I_{\max} + I_{\min}) = |g^{(1)}(\tau)|$.[21] Therefore, the coherence time of the fundamental mode at a certain power can be obtained from the evolution of the visibility $V(\tau)$ with increasing delay times τ. An example of such highly resolved interference fringes is shown in the inset of Fig. 2, with more than 95% visibility around zero delay. We have carried out such visibility measurements at different pump powers covering the transition regime between spontaneous to dominating stimulated emission depicted in Fig. 1(b). The experimental results from the fundamental-mode emission of the 2.6 μm pillar are presented in Fig. 2. A clear qualitative change in the visibilities from a Gaussian-type profile to a more exponential behavior can be observed within the transition regimes of all investigated micropillars. This change in the visibility curves has been verified by calculations based on a semiconductor model (discussed below).

The decay of the first-order coherence function in Fig. 2 gives direct access to the coherence time

$$\tau_c = \int_{-\infty}^{\infty} |g^{(1)}(\tau)|^2 d\tau. \tag{2}$$

The extracted excitation power dependence of the fundamental-mode coherence time for each micropillar is

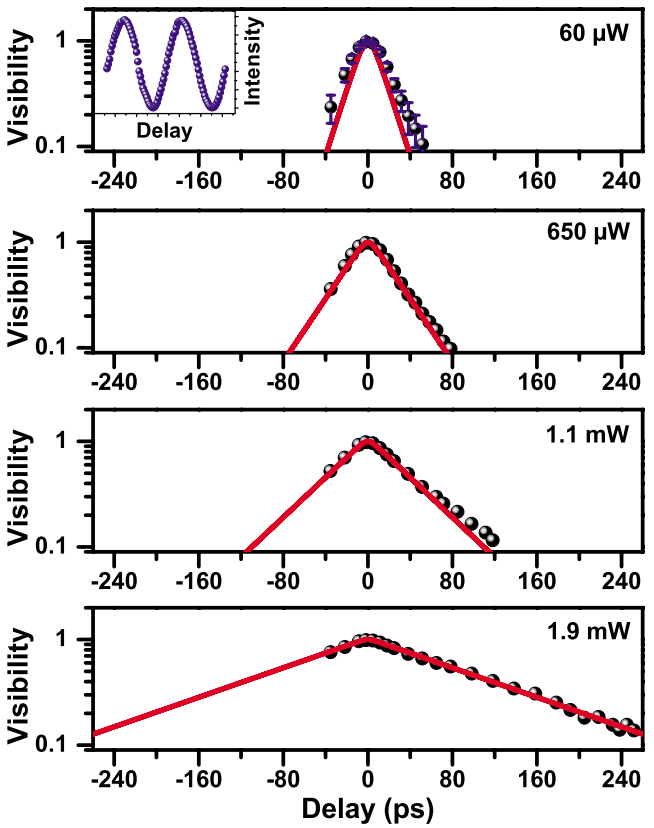

FIG. 2. (Color online) Visibility curves of the fundamental-mode emission from the 2.6 μm pillar at different excitation powers. A gradual change in the visibility profile from Gaussian-type behavior to a more exponential behavior is obtained with increasing excitation power. The measured results (dots) are in qualitative agreement with the calculation (solid lines). Inset: A typical high-resolution interference fringe from the fundamental mode at a certain delay time with $V(\tau)$ over 95%.

displayed in Fig. 3. Interference measurements at low pump powers yield Gaussian-type $V(\tau)$ traces with coherence times of around $\tau_c = 20-30$ ps, thus giving $\Delta E_{\mathrm{FWHM}} = \sqrt{2 \ln 2}/\pi\tau_c^{-1} = 140-90$ μeV for the corresponding emission linewidths—consistent with our spectral data. A nonlinear increase from $\tau_c \approx 30$ to ≈ 990 ps for the 6 μm pillar is observed near and above the transition region from spontaneous into mainly stimulated emission.

A central result of our investigation is that the coherence time τ_c depends strongly on the spontaneous emission coupling β. For the 6 μm pillar (β=0.01), the longest achievable coherence length is $l_c = c\tau_c \approx 30$ cm, whereas significantly smaller values of $l_c \approx 7.5$ cm ($\beta_{2.6\ \mu\mathrm{m}} = 0.03$) and ≈ 3 cm ($\beta_{1.8\ \mu\mathrm{m}} = 0.05$) can be obtained from the smaller-sized structures. To highlight this feature, a calculation of various β values is presented in Fig. 4. Except for β and the number of emitters, the parameters are the same for all three curves (see the figure caption). For comparable points on the i/o curves regarding the threshold, we find that devices with a larger β factor exhibit shorter coherence times. At the same time, even in the case of β=1 (often considered as "thresholdless" laser), the slower but nevertheless distinct rise in the coherence time can be used to identify the threshold region.

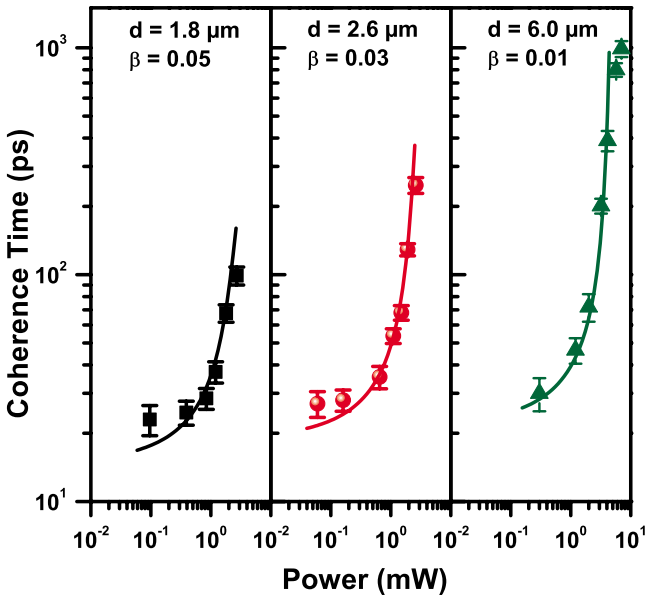

FIG. 3. (Color online) Pump power dependence of the coherence time τ_c of the fundamental-mode emission for 1.8 (squares), 2.6 (spheres), and 6 μm (triangles) pillars in a log-log plot. A nonlinear increase in coherence time is observed for all pillars. As depicted in the figure, longer coherence times were observed for low-β pillars. Excellent agreement with the calculation (solid lines) is presented. Theoretical results are shifted to match the milliwatt scale of the experiment.

The physical origin of the reduced coherence time (increased linewidth) with increasing β is the stronger contribution of spontaneous (incoherent) processes coupled into the laser mode.

A semiconductor theory for the QD emission has previ-

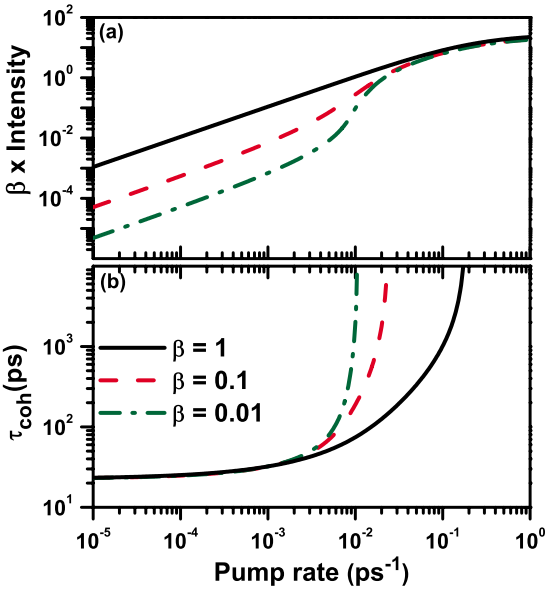

FIG. 4. (Color online) Theoretical i/o curves (top) and coherence times (bottom) for various values of the β parameter. The curve for β=0.01 equals that of the 6 μm pillar. For β=0.1 and β=1, 50 and 5 QDs have been used, respectively. All other parameters remain unaltered.

ously been used to calculate the i/o characteristics and second-order coherence $g^{(2)}(\tau=0)$ at zero delay time of QD-micropillar lasers.[3,17] For the present results we extend the theory to calculate the first-order coherence $g^{(1)}(\tau)$ at *different* delay times.

To obtain the coupled laser equations, we start from a many-body Hamiltonian containing the free-carrier spectrum, the free electromagnetic field, and Coulomb and light-matter interactions. Carriers are treated in second quantization and also the light field is quantized. We consider observables such as the photon number in the laser mode $\langle b^\dagger b\rangle$; the electron and hole populations $\langle c_\nu^\dagger c_\nu\rangle$ and $1-\langle v_\nu^\dagger v_\nu\rangle$, where the index denotes the localized QD states; and the first-order correlation function according to Eq. (1). Using Heisenberg's equations of motion (eoms), the dynamics of these observables is determined. Due to the two-particle parts in the Hamiltonian, a hierarchy problem arises, i.e., in the eom for averages of n particles, $(n+1)$-particle averages appear. This hierarchy is truncated by using the cluster expansion method.[19,22] The application of this method to obtain the semiconductor laser equations was elaborated in Ref. 17.

For the calculation of two-time quantities such as $g^{(1)}(\tau)$ in Eq. (1), we now formulate eom with respect to the delay time τ. This leads to the occurrence of more operator averages with mixed time arguments, i.e., $\langle b^\dagger(t)v_\nu^\dagger(t+\tau)c_\nu(t+\tau)\rangle$. With $g^{(1)}(\tau)$ being a doublet quantity (two-particle average) in the cluster expansion scheme, we truncate the hierarchy consistently at the same level. In comparison, for the calculation of $g^{(2)}(\tau=0)$, which is a quadruplet quantity (four-particle average), the inclusion of averages up to the four-particle level is necessary.

By using the following approximations, an *analytical solution* for $g^{(1)}(\tau)$ can be obtained: (i) stimulated emission is restricted to a single mode, (ii) correlations between photons and charge carriers are neglected ("semiclassical factorization"), (iii) N identical QDs are considered to be in resonance with the laser mode, and (iv) Coulomb effects are included via effective light-matter coupling and scattering rates. With this we find an analytical solution of the form

$$|g^{(1)}(\tau)| = \frac{-\gamma_-}{\gamma_+-\gamma_-}e^{-\gamma_+|\tau|} + \frac{\gamma_+}{\gamma_+-\gamma_-}e^{-\gamma_-|\tau|}, \tag{3}$$

with $\hbar\gamma_\pm = (\kappa+\Gamma)/2 \pm \sqrt{|g|^2N(f^c-f^v)+(\kappa-\Gamma)^2/4}$. Here, $2\kappa/\hbar$ is the cavity loss rate obtained from the Q factors, Γ is the homogeneous QD broadening, and $|g|^2=\hbar(\kappa+\Gamma)\beta/(2\tau_{\text{spont}})$ is the light-matter coupling strength. The stationary populations of the lowest confined QD states f^c and f^v are obtained from the stationary solutions of the dynamic laser equations. From Eq. (2) and the equations above, we find for the coherence time

$$\tau_c = \frac{1}{\gamma_+} + \frac{1}{\gamma_-} + \frac{\hbar}{\kappa+\Gamma}. \tag{4}$$

Equations (3) and (4) have been used to obtain the results shown in Figs. 2–4. As can be seen, the theory predicts the coherence times and line shapes of the visibilities very well. Expanding Eq. (3) in a Taylor series reveals the Gaussian-type characteristic in the decay of $|g^{(1)}(\tau)|$, as the term linear in τ drops out. Contrary to earlier presumptions,[4] this line shape is not caused by the inhomogeneous broadening, but is a consequence of the quantum-mechanical interaction processes. Considering the solutions $\gamma_\pm$ at transparency, $f^c-f^v=0$, we get $\gamma_+=\Gamma \gg \gamma_-=\kappa$, yielding a decay that is close to exponential $|g^{(1)}(\tau)|=e^{-\gamma_-\tau}$.

In conclusion, we have presented a comprehensive study of the first-order coherence in QD micropillar lasers. A steep increase in the coherence time is found around the laser transition, which is accompanied by a change in the decay characteristics of $g^{(1)}(\tau)$ from Gaussian type to exponential. All presented results reveal high conformity with a microscopic laser theory, which has been extended in this work to calculate the two-time correlation function $g^{(1)}(\tau)$.

We gratefully acknowledge financial support from the DFG research group "Quantum optics in semiconductors" and a grant for CPU time at the Forschungszentrum Jülich (Germany).

*Corresponding author; serkan.ates@ihfg.uni-stuttgart.de

[1] F. De Martini and G. R. Jacobovitz, Phys. Rev. Lett. **60**, 1711 (1988).
[2] S. Reitzenstein, A. Bazhenov, A. Gorbunov, C. Hofmann, S. Münch, A. Löffler, M. Kamp, J. P. Reithmaier, V. D. Kulakovskii, and A. Forchel, Appl. Phys. Lett. **89**, 051107 (2006).
[3] S. M. Ulrich, C. Gies, S. Ates, J. Wiersig, S. Reitzenstein, C. Hofmann, A. Löffler, A. Forchel, F. Jahnke, and P. Michler, Phys. Rev. Lett. **98**, 043906 (2007).
[4] S. Ates, S. M. Ulrich, S. Reitzenstein, A. Löffler, A. Forchell, and P. Michler, Appl. Phys. Lett. **90**, 161111 (2007).
[5] S. L. McCall, A. F. J. Levi, R. E. Slusher, S. J. Pearton, and R. A. Logan, Appl. Phys. Lett. **60**, 289 (1992).
[6] P. Michler, A. Kiraz, Lidong Zhang, C. Becher, E. Hu, and A. Imamoglu, Appl. Phys. Lett. **77**, 184 (2000).
[7] J. Renner, L. Worschech, A. Forchel, S. Mahapatra, and K. Brunner, Appl. Phys. Lett. **89**, 231104 (2006).
[8] O. Painter, R. K. Lee, A. Scherer, A. Yariv, J. D. O'Brien, P. D. Dapkus, and I. Kim, Science **284**, 1819 (1999).
[9] H. G. Park, S. H. Kim, S. H. Kwon, Y. G. Ju, J. K. Yang, J. H. Baek, S. B. Kim, and Y. H. Lee, Science **305**, 1444 (2004).
[10] S. Strauf, K. Hennessy, M. T. Rakher, Y. S. Choi, A. Badolato, L. C. Andreani, E. L. Hu, P. M. Petroff, and D. Bouwmeester, Phys. Rev. Lett. **96**, 127404 (2006).
[11] M. Nomura, S. Iwamoto, N. Kumagai, and Y. Arakawa, Phys. Rev. B **75**, 195313 (2007).
[12] A. Löffler, J. P. Reithmaier, G. Sek, C. Hoffmann, S. Reitzentein, M. Kamp, and A. Forchel, Appl. Phys. Lett. **86**, 111105 (2005).
[13] D. Birkedal, K. Leosson, and J. M. Hvam, Phys. Rev. Lett. **87**, 227401 (2001).

[14] C. Kammerer, C. Voisin, G. Cassabois, C. Delalande, P. Roussignol, F. Klopf, J. P. Reithmaier, A. Forchel, and J. M. Gérard, Phys. Rev. B **66**, 041306(R) (2002).
[15] B. Gayral, J. M. Gérard, G. Legrand, E. Costard, and V. Thierry-Mieg, Appl. Phys. Lett. **72**, 1421 (1998).
[16] S. Reitzenstein, C. Hofmann, A. Gorbunov, M. Strauss, S. H. Kwon, C. Schneider, A. Löffler, S. Höfling, M. Kamp, and A. Forchel, Appl. Phys. Lett. **90**, 251109 (2007).
[17] C. Gies, J. Wiersig, M. Lorke, and F. Jahnke, Phys. Rev. A **75**, 013803 (2007).
[18] M. Schwab, H. Kurtze, T. Auer, T. Berstermann, M. Bayer, J. Wiersig, N. Baer, C. Gies, F. Jahnke, J. P. Reithmaier, A. Forchel, M. Benyoucef, and P. Michler, Phys. Rev. B **74**, 045323 (2006).
[19] N. Baer, C. Gies, J. Wiersig, and F. Jahnke, Eur. Phys. J. B **50**, 411 (2006).
[20] B. Gayral, J. M. Gérard, A. Lemaitre, C. Dupuis, L. Manin, and J. L. Pelouard, Appl. Phys. Lett. **75**, 1908 (1999).
[21] R. Loudon, *The Quantum Theory of Light* (Oxford University Press, New York, 2000).
[22] J. Fricke, Ann. Phys. (N.Y.) **252**, 479 (1996).